Detection of HF First-Order Sea Clutter and Its Splitting Peaks with Image Feature: Results in Strong Current Shear Environment

Yang Li[1], Zhenyuan Ji[1], Junhao Xie[1], and Wenyan Tang[2]

[1] Department of Electronic Engineering, [2] Institute of Automatic Testing and Control
Harbin Institute of Technology
Harbin 150001, China
li.yang@hit.edu.cn

Abstract. Strong current shear environment always results in the twisty and splitted sea clutter along the range dimension in the range-Doppler spectral map. A sea clutter detection method with image feature is proposed. With 2-D image features in range-Doppler spectrum, the trend of first-order sea echoes is extracted as indicative information by a multi-scale filter. Detection rules for both single and splitting first-order sea echoes are given based on the characteristic knowledge combining the indicative information with the global characteristics such as amplitude, symmetry, continuity, etc. Compared with the classical algorithms, the proposed method can detect and locate the first-order sea echo in the HF band more accurately especially in the environment with targets/clutters smearing. Experiments with real data in strong current shear environment verify the validity of the algorithm.

Keywords: sea state remote sensing; first-order sea clutter; image feature; Bragg peak splitting; high frequency radar.

1 Introduction

In the application of sea state remote sensing, High Frequency Surface Wave Radar (HFSWR) acquires the sea state information by estimating the parameters of the first order and second order sea echo/clutter. On the other hand, in the surveillance of moving target such as ship and iceberg, it will result in the false alarm and missing alarm for not recognizing targets and sea clutter when the speed of them is equal or close. Thus, it is a key and useful technique to detect the first-order sea echo (clutter/backscatter) spectra (Bragg Peak) contaminated with clutter/noise not only for sea state sensing but also for long range target detection [1,2]. In most surveillance space for HFSWR, the Bragg peaks near the coast are always dominant in local Doppler spectrum. Thus Hickey and Gill proposed a local peak detection method [3]. And Barrick gave the statistical location of the first-order sea echo by estimating the centroid of spread spectrum peaks [4]. However, if there are ships, ionosphere

J. Blanc-Talon et al. (Eds.): ACIVS 2012, LNCS 7517, pp. 503–514, 2012.

interference[5] and other clutters around the Bragg peak, the performances of those algorithms will be degraded rapidly [6]. To solve the problems, clutter canceling methods are proposed using space-time characteristics to eliminate/extract first-order sea clutters from interferences [7-9]. To get a better detection performance, Ji analyzed characteristics and mechanism of first-order sea clutters systematically [10]. And Tong studied a ship target CFAR detection method in a strong sea clutter background with the amplitude characteristic and background distribution information [11]. In literature [12], four detection rules for Bragg peak location were proposed based on multidimensional characteristics such as amplitude, SNR (signal-to-noise ratio), continuity, symmetry, etc., which solved the Bragg peak detection problem to some extent. Recent researches [13,14] found that Bragg peak spectrum would be migrated, spread or splitting when there was strong current shear, eddy or some other interrupted current changes. In such circumstances, sea environment parameters estimation and target detection performances will be decreased if there is no way to identify them.

In this paper, a method with image feature is proposed to detect HF first-order sea echoes. After the theory of the first-order sea clutter in the HF band is introduced, the trend of Bragg peaks in range-Doppler map is extracted by image feature in multi-scale space. Combining the trend information with the experiential knowledge, rules for detecting both single and splitting Bragg peaks are given. Then the flow chart shows the procedure of the algorithm. In the experiments, real data Strong current shear environment is used for verifying the validity of the proposed method

2 First-Order Sea Echo in the HF Band

Lots of experiments show that the backscatter of sea surface has specific Doppler shift correlating with sea state by HF irradiation when the sea is fully developed. Crombie observed the phenomena and deduced first-order interaction between HF electromagnetic wave and ocean wave with Bragg scattering model [15]. This theory indicates that the dominant symmetrical spikes (namely first-order Bragg peaks of sea clutter) in Doppler spectrum are generated by double sets of sea wave trains with $\lambda/2$ (where λ is the radar wavelength) moving forward and receding from the radar. In deep water, the predicted position of the first-order Bragg peak is

$$f_B = \pm\sqrt{\frac{g}{\pi\lambda}} = \pm\sqrt{\frac{gf_c}{\pi c}} \tag{1}$$

Here, f_c is the radar carrier frequency, g is the gravitational constant, and c is the velocity of light. Considering the shallow sea, the above formula can be modified as

$$f_B = \pm\sqrt{\frac{gf_c}{\pi c}\tanh(\frac{4\pi hf_c}{c})} \tag{2}$$

Here, h is the water depth, $\tanh(\cdot)$ is the hyperbolic tangent function. Simulation shows that if f_c >2MHz and h<30m, the results from (1) and (2) tend to be uniform [13].

From the actual measurements, it can be found that the locations of first-order peaks often departure from the theoretical values (see Figure1(a)). The reason is that the waves causing first-order scattering are superimposed on a sea surface which are physically moving due to surface currents [16]. The radial component of this surface-current vector can thus be calculated in terms of the offset of the Bragg peak.

Under normal conditions, the effect on the position of the Bragg peak by the surface-current is stable. In that case, the surface current field is homogenous in radar target spatial resolution, and the Bragg peak is shown as a narrow-band single spike. Heron and Gill [16] found that Bragg peak splitting was induced by the non-uniform velocity field within the target cell resulting from strong current shear and eddy. A typical example is shown in Figure1(a).

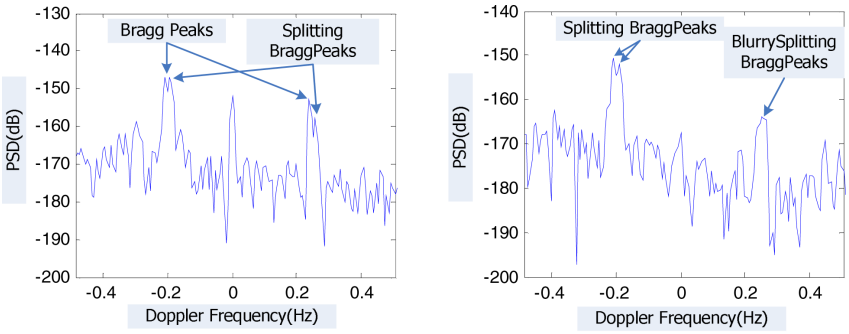

Fig. 1. Doppler spectrum of HFSWR: (a) Typical Doppler spectrum, (b) Blurry splitting Bragg peaks

What's more, ship echoes, ionosphere interference, radio frequency interference and second-order continuum, etc. can also contaminate the first-order spectrum. It's obvious that the actual situation for Bragg peaks is more complicated than the case in which the amplitude is dominant and the position is predictable. We can conclude that, to locate the first-order sea echo spectrum accurately in such a changeable environment, invariant features making the Bragg peak distinctive from other echoes should be found firstly.

3 Location of the Bragg Peak

3.1 Spectral Characteristics of the Bragg Peak

Experimental measurements show that the first-order sea echoes have these features in stable ocean surface current in the distance not far from the coast (usually less than 200km):

1) The offset range between the theoretical value and the actual measurement is predictable [4].

2) The offset directions of the positive/negative Bragg peaks in a same range bin are same [16].
3) The Bragg peak is dominant in Doppler spectrum which is presented as local maximal or the 2nd major amplitude. The windowing Bragg peak usually occupies 3-5 spectral lines.
4) Because the motion of sea surface is continuous, the position of the Bragg peak is changing slowly and continuously along the range direction.
5) The SNR being used for estimating the radial surface current is above 5-10dB [12].

If there are no ships, ionosphere interference and strong current shear near the Bragg peak, the above characteristics can be used for detecting Bragg peaks with a good performance.

If there are no ships, ionosphere interference and strong current shear near the Bragg peak, the above characteristics can be used for detecting Bragg peaks with a good performance.

3.2 Multi-scale Filter and Image Feature Extraction

In Amplitude-Range-Doppler (ARD) spectrum of HFSWR (see Figure2), first-order sea echoes in the gray image of RD spectrum is presented as two dominant, symmetrical and smooth curves. It results from Bragg resonance and symmetry effect to the sea surface by the ocean current. The offset of the first-order sea echo varies with the range bins especially in the region far from the coast. Let's take the real data shown in Figure2 as an example. The relative position offset of Bragg peak between the measurement and the theoretical value varies from -0.026Hz to 0.026 Hz. If searching range centering at the theoretical value is $[-\Delta_{\max}, \Delta_{\max}]$ (where $\Delta_{\max}$ is the velocity offset causing by the maximal radial ocean current, and $\Delta_{\max}$=0.026Hz in that example), it will lead to too much candidate peaks that results in error detection or false alarms. It's obvious that the two Bragg lines along the range are presented as ridges in the gray image of RD spectrum. Thus a certain image processing method is proposed to help extract Bragg peaks in the rang-Doppler plane.

First of all, multi-scale filter is used for filtering the high frequency noise in ARD map. Given any image $f: R^2 \times \to R$, its scale-space representation $L: R^2 \times R_+ \to R$ is defined by [17]

$$L(\cdot;t) = g(\cdot;t) * f \tag{3}$$

Where $*$ denotes convolution, $g: R^2 \times R_+ \to R$ denotes the Gaussian kernel given by

$$g(x, y; t) = \frac{1}{2\pi t} e^{-(x^2+y^2)/(2t)} \tag{4}$$

and t is the scale parameter, (x, y) denotes the Cartesian coordinates of a certain point in the 2-D image. From this representation, scale-space derivatives are then defined by

$$L_{x^\alpha y^\beta}(\cdot;t) = \partial_{x^\alpha y^\beta} L(\cdot;t) = g_{x^\alpha y^\beta}(\cdot;t) * f \tag{5}$$

Here (α,β) is the order of differentiation. It's easy to find that filtering results vary from different t.

Then use a ridge detection method for extracting Bragg peaks from filtered ARD image. We can give a relative wider range for ridge detection according to the maximal offset by ocean current in radar detection area. And calculate the 1st and the 2nd order differentiation $L_{x^1y^0}(v,r;t)$ and $L_{x^2y^0}(v,r;t)$ at (v,r) along the Doppler dimension (where v is the Doppler bin number and r is the range bin number). If

$$\begin{cases} L_{v^1r^0}(v,r;t)L_{v^1r^0}(v,r+1;t)<0 \\ L_{v^2r^0}(v,r;t)<0 \end{cases} \text{ or } \begin{cases} L_{v^1r^0}(v,r;t)L_{v^1r^0}(v,r-1;t)<0 \\ L_{v^2r^0}(v,r;t)<0 \end{cases} \tag{6}$$

The point (v,r) is defined as a ridge. The above processing results sometimes involve both Bragg peaks and other interference (such as ionosphere, ships, etc.). Because the interference is relative positional independent in RD map, we can use one of morphologic processing methods, called erosion [18], for filtering them.

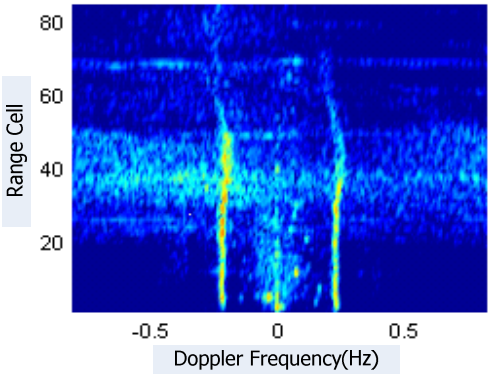

Fig. 2. ARD spectrum

Figure3 is the processing result which takes Figure2 as the original input data. Let t=22. We can summarize the characteristics of Bragg peaks in strong current shear environment:

1) In range bin 70-80 being far from the coast, because those positive Bragg peaks are smeared by the effect of surface wave attenuation and ionosphere interference.
2) The positions of Bragg peaks deviate from the theoretical in strong current shear environment. And such bias shows the irregular trend along the range dimension in RD map.

3) Splitting peaks appear (from No.37-70 range cells) in high frequency as a result of the effect of strong current shear.

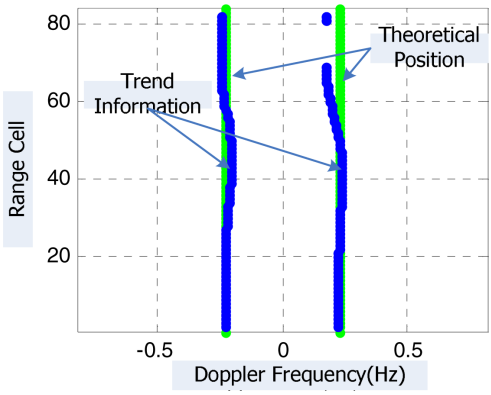

Fig. 3. Trend of Bragg peaks

3.3 Global Rules for Bragg Peak Extraction

Based on the former results, rules for Bragg peak extraction is given as

1) Spectral characteristic criterion Set detection band $[v_0 - \Delta_{\max}, v_0 + \Delta_{\max}]$ in Doppler region at (v_0, r_i). Select local peaks in the detection band as candidate Bragg peaks. The number of reference cells can be 2-4. The initial screening position (v_0, r_i) is determined by the trend information of Bragg peaks that has been got in Section 2.2.
2) Symmetry criterion Compare the positions of positive with negative candidate peaks at a same range bin, and pick up the ones that offset symmetrically.
3) Continuous and smooth criterion As the simplest smooth curve, cubic spline is used for getting secondary indicative information of Bragg peaks from candidate peaks. In this way, continuous and smooth indicative information can be got in the range direction.
4) SNR criterion Use the SNR estimation method which is able to eliminate interference, clutters, etc. in reference cells. Then reject the target of which SNR is less than 6dB.

3.4 Global Rules for Bragg Peak Extraction Splitting Bragg Peak

In middle Doppler resolution (integrating time is about 100-200s), as well-known phenomena for HFSWR, Bragg peak splitting is resulted from a transient change of a surface current field within a target cell. In this paper a Bragg peak with bigger amplitude in any side of zero Doppler is called primary peak; a smaller one near the primary peak is called splitting peak which still satisfies most characteristics in

Section 2.1. The amplitude difference between primary peak and splitting peak at the same side of zero Doppler in the same range bin (usually 0-20dB) varies with the relative position between the current shear and the target cell. We also found that the smaller the SNR of splitting peak is, the more seriously the detection performance is affected by interference. In this paper, it's called blurry splitting Bragg peaks, which are presented as visible on the positive/negative side but invisible on the other side of zero Doppler(see Figure1(b)).

Basing on the observation and mechanism of splitting Bragg peaks, detection rules are given as

1) *Second largest criterion*
   In local area Splitting Bragg peak is dominant in local area in Doppler region except for the primary peak.
2) *Offset range prediction criterion*
   The distance between a primary peak a the splitting peak should be no more than $\Delta'_{\max}$ (where $\Delta'_{\max}$ is the maximal Doppler offset of Bragg peaks causing by the stable/transient current). Thus the searching range for splitting Bragg peaks is $[f_m - \Delta'_{\max}, f_m + \Delta'_{\max}]$, where f_m is the Doppler position of the primary peak.
3) *Symmetry criterion*
   Because current shear acts on both sides of Bragg peaks symmetrically, the offset directions of the positive/negative splitting Bragg peaks in the same range bin are same. Considering resolution, system error, etc., let one Doppler cell be the tolerable error in middle Doppler resolution.
4) *Amplitude difference criterion*
   The amplitude difference between primary peak and splitting peak at the same side of zero Doppler in the same range bin, usually 0-20dB. If the difference exceeds this range, the corresponding targets will be determined as interference.
5) *Blurry splitting Bragg peak identify criterion*
   Interference sometimes makes a splitting peak be visible on only one side of zero Doppler. In this case, it's necessary for us to study the spectrum around the primary peak on the invisible side. If the spectral structure is presented as characteristics interfered by adjacent cells, it can be determined as blurry splitting Bragg peak. The broadening degree of the primary peak can help to identify the phenomena.
6) *SNR criterion*
   Supporting by the SNR estimation algorithm with wild value and identified clutter elimination, a splitting peak should satisfy a specified SNR (for example, 5-10dB). Peaks with too lower SNR are meaningless for current estimation and surface target detection as well.

3.5 Flow Chart of the Algorithm

A simplified detection algorithm flow chart of Bragg peak is shown in Figure4 based on Section 3.1-3.4. Each node in the figure corresponds to the above-mentioned algorithms or rules. Main difference between widely used methods and the proposed

method is marked with dashed frames. On the one hand, the ridge detection algorithm followed by multi-scale filtering gives trend information of Bragg peak in RD map; on the other hand, the splitting Bragg peak detection method provides more accurate and precise sea state information and helps decrease false alarms and missing alarms for sea surface moving target detection.

It must be noted that, being affected by strong clutters and noise, the trend information sometimes cannot locate the position of Bragg peaks accurately. In addition, splitting peaks increase the emergence risk of the false alarm. Thus "blind area" and "global characteristic confirmation" blocks are added to the flow chart. The former aims at investigating the area without indicative trend information and confirm the candidate Bragg peak by symmetry. The latter is aided by both symmetry and smooth criterion to control the false alarm rising from splitting peaks detection, high order sea clutter and ships. Other processes in the algorithm flow diagram can also help get better performances.

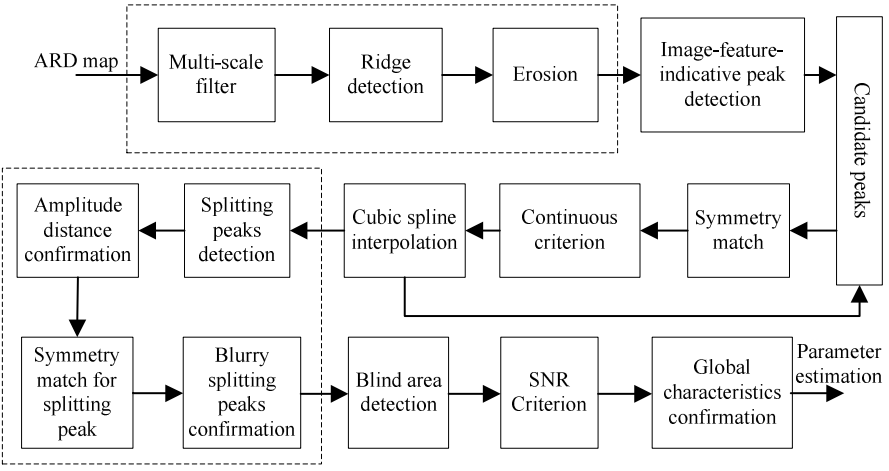

Fig. 4. Flow chart of Bragg peak detection

4 Experiments and Result Analysis

To verify the advantage of the proposed algorithm, three methods have been operated on the same real data from HFSWR. The carrier frequency is 4.9MHz, and the integrated period of Doppler process is 120s. Considering the resolution of HFSWR and the maximal offset by radial current in the detected sea area, select 5 positive/negative Doppler cells as searching area to select candidate Bragg peaks. The positions of the Bragg peaks shown in Figure5 are estimated by the methods in literature [19] after detection.

Figure5 shows the results of the experiments in strong current environment. Method 1 uses criterion 1 in Section 3.3 and local maximal rule to select the maximal

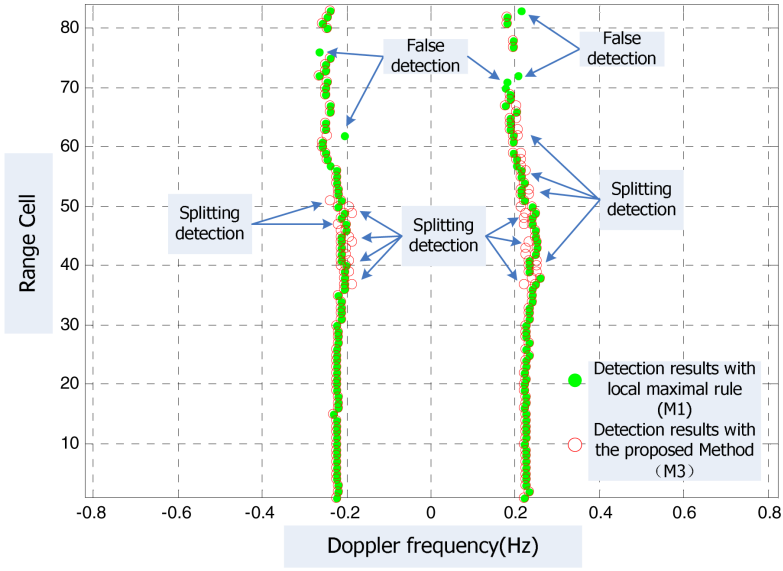

(a)

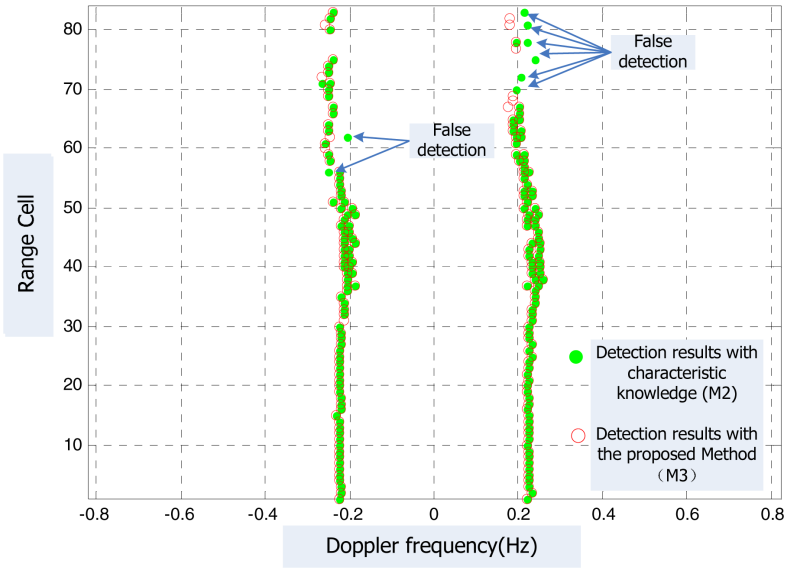

(b)

Fig. 5. Results of detection of Bragg peaks: (a) M1 vs. M3, (b) M2 vs. M3

peak as candidate Bragg peaks. Method 2 is aided with characteristic knowledge which has been noted in Section 3.2-3.3. Method 3 uses the image feature as indicative information (Section 3.1) and characteristic knowledge (Section 3.2-3.3). For convenience in this paper, those methods are called M1, M2 and M3 respectively.

Figure5(a) and (b) show the detection results by M1 vs. M3 and M2 vs. M3 separately. Compared with the original ARD spectrum (Figure 2), we can find that these three methods give the same results in the coastal water (No. 1-35 range cells). The main difference in the strong current environment (No. 37-70 range cells) is the capability of recognizing the splitting peaks.

Experimental data show that for the amplitude of the sea echo in HF band is affected by surface wave attenuation, there are no Bragg peaks detected far from the seashore in the positive Doppler frequency. In such circumstance, M1 and M2 perform their arbitrary property in selecting candidate Bragg peaks. And M3 uses trend information of Bragg peaks in RD map which can help select the proper candidates for the post-process.

We can make a conclusion that

1) The performance of those three methods is same without other echoes such as ionosphere interference, ships, etc. near the coast because the Bragg peaks are dominant in local Doppler region.
2) When other echoes are moving close to Bragg peaks, M1 or M2 cannot identify Bragg peaks well without multi-dimensional features or trend of Bragg peaks in RD map. In those cases, for using indicative information based on image feature, M3 can still detect Bragg peaks correctly.
3) M2 and M3 can extract splitting Bragg peaks and identify blurry splitting peaks to some extent. Limited by the performance of primary peaks detection far from the coast, M2 gives false alarm; M3 is capable of controlling the number of false alarms with a better performance.
4) Compared with the results in weak current environment [20], M3 shows a distinct advantage. The recognition rate of M1, M3 and M3 are 61.9%, 79.8% and 96.4%.

5 Conclusions

To increase the HF first-order sea echo detection performance in clutter/noise environment, a characteristic-knowledge-aided spectrum detection method is proposed. First of all, the ridge feature in multi-scale range-Doppler spectrum is extracted as indicative information. Secondly, combined with amplitude, symmetry, continuity, etc. as global characteristics, detection rules for both single and splitting Bragg peak are presented. Then, the flow chart of the algorithm is given. At last, experiments with real data verify that, compared with the widely used methods, the proposed method can achieve a better detection performance especially in the strong current shear environment. The result can be utilized in both moving target detection and sea state remote sensing.

Acknowledgment. The project is supported by the National Natural Science Foundation of China (Grant No. 61102158), the State Key Program of the National Natural Science Foundation of China (Grant No. 61132005), General Financial Grant from the China Postdoctoral Science Foundation (Grant No. 2011M500667) and the Fundamental Research Funds for the Central Universities (Grant No. HIT.NSRIF.2012022).

References

1. Wyatt, L.R., Green, J.J., Middleditch, A., et al.: Operational Wave, Current, and Wind Measurements With the Pisces HF Radar. IEEE Journal of Oceanic Engineering 31(4), 819–834 (2006)
2. Sevgi, L., Ponsford, A., Chan, H.C.: An Integrated Maritime Surveillance System Based on High-Frequency Surface-Wave Radars, Part 1: Theoretical Background and Numerical Simulations. IEEE Antennas and Propagation Magazine 43(4), 28–43 (2001)
3. Hickey, K.J., Gill, E.W., Helbig, J.A., et al.: Measurement of ocean surface currents using a long-range, high-frequency ground wave radar. IEEE Journal of Oceanic Engineering 19(4), 549–554 (1994)
4. Barrick, D.E.: Accuracy of parameter extraction from sample-averaged sea-echo Doppler spectra. IEEE Transactions on Antennas and Propagation 28(1), 1–11 (1980)
5. Shang, S., Zhang, N., Li, Y.: Research of Ionospheric Clutter Statistical Properties in HFSWR. Chinese Journal of Radio Science 26(3), 521–527 (2011)
6. Wyatt, L.R., Green, J.J., Middleditch, A.: Wave, Current and Wind Monitoring using HF Radar. In: Proc. of the IEEE/OES Eighth Working Conference on Current Measurement Technology, pp. 53–57. IEEE Press, New York (2005)
7. Khan, R., Power, D., Walsh, J.: Ocean Clutter Suppression for An HF Ground Wave Radar. In: IEEE 1997 Canadian Conference on Electrical and Computer Engineering, pp. 512–515. IEEE Press, New York (1997)
8. Wang, J., Lynn, R.K.: Improvement of high frequency ocean surveillance radar using subspace methods based on sea clutter suppression. In: Sensor Array and Multichannel Signal Processing Workshop Proceedings, pp. 557–560. IEEE Press, New York (2002)
9. Xing-Bin, G., Cheng-Ge, Z., Ye-Shu, Y.: Sea-Clutter-Canceling for HF Ground-Wave Shipborne OTH Radar. Dian Zi Xue Bao 28(3), 5–8 (2000)
10. Ji, Z., Meng, X., Zhou, H.: Analysis of Sea Clutters in HF Ground Wave Over-the-Horizon Radar. System Engineering and Electronics 22(5), 12–16 (2000)
11. Tong, J., Wen, B., Wang, S.: Ship Target Detection in Strong Sea Clutter Background. Journal of Wuhan University (Natural and Science Edition) 51(3), 370–374 (2005)
12. Qiang, Y.: Research of Detector in High Frequency Ground Wave Radar, Harbin Institute of Technology (August 2002)
13. Parkinson Murray, L.: Observations of the broadening and coherence of MF lower HF surface-radar ocean echoes. IEEE Journal of Oceanic Engineering 2(2), 347–363 (1997)
14. Heron, M.L., Gill, E.W., Prytz, A.: An Investigation of Double-peaked HF Radar Spectra via A Convolution/De-convolution Algorithm. In: OCEANS 2008, pp. 1–5. IEEE Press, New York (2008)
15. Crombie, D.D.: Doppler Spectrum of Sea Echo at 13. 56MHz. Nature 175, 681–682 (1955)
16. Barrick, D.E., Headrick, J.M., Bogle, R.W., et al.: Sea Backscatter at HF: Interpretation and Utilization of the Echo. Proceedings of the IEEE 62(6), 673–680 (1974)

17. Lindeberg, T.: Edge Detection and Ridge Detection with Automatic Scale Selection. International Journal of Computer Vision 30(2), 107–153 (1998)
18. Yujin, Z.: Image Engineering (II): Image Analysis, 2nd edn., pp. 369–376. Tsinghua University Press, Beijing (2005)
19. Yang, L., Ning, Z., Qiang, Y.: A Fast, Accurate Spectral Peak Location Estimator. Journal of Harbin Institute of Technology 40(S1), 160–163 (2008)
20. Yang, L., Ning, Z., Qiang, Y.: Characteristic-Knowledge-Aided Spectral Detection of High Frequency First-Order Sea Echo. Journal of Systems Engineering and Electronics 20(4), 718–725 (2009)